Frontiers in Bioscience Landmark

Front. Biosci. (Landmark Ed) **2025**; 30(12): 45389
https://doi.org/10.31083/FBL45389

Original Research

SB431542, a Selective Inhibitor of the TGF-β Type I Receptor, Enhances Doxorubicin Antitumor Activity via p63 Activation in Mutant p53 Breast Cancer Cells

Yu-Ling Kou[1,†], Yu-Jie Liu[1,†], Tzu-Chi Hsu[1], Kuan-Yo Wu[2], Sih-Tong Chen[3], Jing-Yan Chen[3], Kuan-Yu Lin[3], Hsiao-Hsuan Wang[3], Yi-Ting Cheng[3], Chia-Chi Chen[4,5,6,*], Bi-He Cai[7,*]

[1]Department of Medical Laboratory Science, I-Shou University, 82445 Kaohsiung, Taiwan
[2]Department of Biomedical Engineering, I-Shou University, I-Shou University, 82445 Kaohsiung, Taiwan
[3]Department of Medical Science and Biotechnology, I-Shou University, 82445 Kaohsiung, Taiwan
[4]Department of Pathology, E-Da Hospital, 82445 Kaohsiung, Taiwan
[5]Department of Physical Therapy, I-Shou University, 82445 Kaohsiung, Taiwan
[6]Department of Occupational therapy, I-Shou University, 82445 Kaohsiung, Taiwan
[7]School of Medicine, I-Shou University, 82445 Kaohsiung, Taiwan
*Correspondence: sasabelievemydream@gmail.com (Chia-Chi Chen); bigbiha@isu.edu.tw (Bi-He Cai)
[†]These authors contributed equally.

Academic Editor: Jordi Sastre-Serra
Submitted: 29 July 2025 Revised: 27 November 2025 Accepted: 3 December 2025 Published: 18 December 2025

Abstract

Background: *TP53* gene mutations are common in breast cancer and are linked to chemoresistance. *p63*, a p53 family member, can induce apoptosis independently of p53, representing a potential therapeutic target in *TP53*-mutant tumors. This study evaluated the synergistic effects of SB431542, a TGF-β type I receptor inhibitor, and doxorubicin in *TP53*-mutant breast cancer cells. **Methods**: Isoform-specific RT-PCR was used to assess TAp63 and ΔNp63 expression following SB431542 treatment in T47D, MDA-MB-231, and MDA-MB-468 cells. Cell viability was assessed using the CCK8 assay. Synergistic interaction was quantified using the Coefficient of Drug Interaction (CDI). Caspase-3/7 activity assays and immunocytochemistry analyses were performed to evaluate apoptotic signaling and p63 expression. Inhibition studies using PETα, a p53-family inhibitor, and a pan-caspase inhibitor were conducted to determine the pathway dependency of the observed effects. **Results**: SB431542 selectively increased TAp63 but not ΔNp63 expression in all three *TP53*-mutant breast cancer cells. GAS6, a TAp63 target, was also upregulated by SB431542. Treatment with SB431542 and doxorubicin used in combination significantly reduced cell viability (CDI 0.54–0.63), increased caspase activity, and enhanced p63 expression. The anticancer effect was significantly reduced by co-treatment with either the p53-family inhibitor or the pan-caspase inhibitor, confirming that the cytotoxic response was mediated through TAp63 and caspase activation. **Conclusions**: SB431542 potentiates doxorubicin-induced apoptosis in *TP53*-mutant breast cancer cells by upregulating TAp63 and activating caspase-dependent pathways. These findings suggest that targeting the TGF-β/TAp63 signaling axis may offer a novel therapeutic approach to overcome chemoresistance in aggressive, *TP53*-mutant breast cancers.

Keywords: SB431542; doxorubicin; p63; tumor suppressor protein p53; mutation; breast cancer; drug interactions

1. Introduction

SB431542 is a selective inhibitor of the TGF-β type I receptor (ALK5), which effectively blocks the TGF-β/Smad2/3 signaling cascade [1]. SB431542 has been widely used in studies of cell differentiation and reprogramming. It facilitates the maintenance of pluripotency and promotes directed differentiation by modulating TGF-β signaling, as demonstrated in embryonic stem cells [2,3]. In the context of cancer biology, SB431542 has been used to study the role of TGF-β signaling in tumor progression and epithelial-to-mesenchymal transition (EMT). For example, Halder *et al*. [4] showed that SB431542-mediated inhibition of TGF-β suppresses EMT and reduces invasiveness in mammary tumor cells. Beyond its classical roles, SB431542 has also been shown to modulate transcription factor networks. Notably, it induces TAp63 expression in human embryonic stem cells [5]. Furthermore, a recent study demonstrated that SB431542 upregulates TAp63 in HaCaT keratinocytes carrying two mutant p53 alleles (R282Q and H179Y), highlighting its broader role in activating the p63 pathway under mutant p53 conditions [6].

p63 exists in multiple isoforms, some with transactivation domains (TAp63) and others without (ΔNp63), which have differing or even opposing functions [7,8]. TAp63, a transactivation-competent isoform of p63, functions as a tumor suppressor and shares structural and functional similarities with p53, a member of the p53 family with an N-terminal transactivation domain that can induce canonical

Copyright: © 2025 The Author(s). Published by IMR Press.
This is an open access article under the CC BY 4.0 license.

Publisher's Note: IMR Press stays neutral with regard to jurisdictional claims in published maps and institutional affiliations.

p53 target genes [9,10]. TAp63 plays a critical role in inducing cell cycle arrest, apoptosis, and the DNA damage response in p53-mutant or dysfunctional cells and exhibits p53-like tumor-suppressive activity [11]. Restoration or activation of TAp63 has been shown to suppress tumor growth and metastasis in mouse models by inducing senescence and activating DNA repair genes [12]. Therefore, pharmacological activation of TAp63 represents a promising therapeutic strategy for mutant p53 tumors [13,14]. Studies indicate that doxorubicin induces TAp63 expression in some cancer cell lines, suggesting a compensatory tumor suppressor role in the absence of wild-type p53 [15,16]. Specifically, TAp63 enhances chemosensitivity by promoting apoptosis in response to doxorubicin, thereby inhibiting tumor progression [16].

In this research, we investigated the potential anticancer effects of SB431542, a selective ALK5 inhibitor, in combination with doxorubicin in mutant p53 breast cancer cells. SB431542 effectively inhibits TGFβ/Smad signaling, which plays a central role in tumor progression and metastasis [4]. Moreover, doxorubicin, while a cornerstone of breast cancer therapy, is often limited by resistance and cardiotoxicity [17–19]. We hypothesized that SB431542 would enhance doxorubicin efficacy in mutant p53 cells, which frequently exhibit chemoresistance [20]. This approach has the potential to overcome drug resistance and improve outcomes in aggressive breast cancers.

2. Materials and Methods

2.1 Cell Culture and Drug Treatment

Human breast cancer cell lines T47D, MDA-MB-231 and BT-474 were obtained from the Bioresource Collection and Research Center (BCRC, Hsinchu, Taiwan), while MDA-MB-468 cells were acquired from the American Type Culture Collection (ATCC, Manassas, VA, USA). Cells were cultured at 37 °C in a humidified atmosphere containing 5% CO_2. MDA-MB-231 and MDA-MB-468 cells were maintained in Dulbecco's Modified Eagle Medium (DMEM; Invitrogen, Carlsbad, CA, USA), whereas T47D cells were grown in RPMI-1640 medium (Invitrogen, Carlsbad, CA, USA). BT-474 were maintained in Hybri-Care Medium (ATCC, Catalog No. 46-X). All media were supplemented with 10% fetal bovine serum (FBS; Invitrogen), 100 U/mL penicillin, and 100 µg/mL streptomycin (Invitrogen). All cell lines were validated by STR profiling and tested negative for mycoplasma. Drug treatments included: vehicle control (DMSO), SB431542 (20 µM; MedChemExpress, Monmouth Junction, NJ, USA), doxorubicin (1 µM; Sigma-Aldrich, St. Louis, MO, USA), PETα (5 µM; p53-family inhibitor; MedChemExpress), and z-VAD-FMK (20 µM; pan-caspase inhibitor; MedChemExpress).

2.2 Cell Viability Assay (CCK-8)

Cell viability was determined using the CCK-8 assay (Invitrogen). CCK-8 reagent (10 µL) was added to each well of a 96-well plate, and the plate was incubated at 37 °C in a CO_2 incubator for 1 h. Absorbance was measured at 450 nm using a SpectraMax iD3 microplate reader (Molecular Devices, Silicon Valley, CA, USA). Wells containing only medium (no cells) were used as blanks. Cells treated with DMSO served as the reference control and were set as 100% viability for normalization. Cell viability (%) was calculated using the formula: [(OD(Drug) – OD(Blank))/(OD(control) – OD(Blank))] $\times$ 100.

2.3 Drug Interaction Analysis

Drug interaction was assessed using the coefficient of drug interaction (CDI), calculated as: CDI = AB/(A $\times$ B) [21], where AB represents the viability ratio of the combination treatment group, and A and B represent the ratios of the individual treatments relative to the DMSO control. CDI values were interpreted as follows: CDI $<$1, synergistic; CDI = 1, additive; CDI $>$1, antagonistic. A CDI $<$0.7 was considered a strong synergistic effect [22].

2.4 Quantitative Real-Time RT-PCR

Total RNA was extracted using TRIzol reagent (Invitrogen). For cDNA synthesis, 1 µg of RNA was reverse transcribed with the QuantiNova Reverse Transcription Kit (Qiagen, Hilden, Germany). Quantitative PCR was performed using HOT FIREPol EvaGreen qPCR Mix Plus (Omics Bio, New Taipei City, Taiwan) and gene-specific primers on a CFX Duet Real-Time PCR System (Bio-Rad, Hercules, CA, USA). Relative gene expression was calculated using the $2^{-\Delta\Delta CT}$ method, with GAPDH as the internal control. Primer sequences were: *GAPDH*: F 5′-GTCTCCTCTGACTTCAACAGCG-3′, R 5′-ACCACCCTGTTGCTGTAGCCAA-3′; *TAp63*: F 5′-TGTATCCGCATGCAGGACT-3′, R 5′-CTGTGTTATAGGGACTGGTGGAC-3′; Δ*Np63*: F 5′-GAAAACAATGCCCAGACTCAA-3′, R 5′-TGCGCGTGGTCTGTGTTA-3′; *GAS6*: F 5′-CCAAAAACTCAGGCTTCGCC-3′, R 5′-AGAAGTTGCCCATGAGGTCC-3′

2.5 Immunocytochemistry

Cells were washed twice with PBS and fixed in 4% paraformaldehyde (100 µL per well) for 20 min. After two washes with wash buffer (1% BSA in PBS), cells were blocked with 1% BSA and 0.2% Triton X-100 in PBS for 30 min. Primary antibody against p63α (sc-8344; Santa Cruz Biotechnology, Dallas, Texas, USA; 1:200 dilution in blocking buffer) was applied for 2 h at room temperature. Cells were washed three times and incubated with PE-conjugated secondary antibody (406421; BioLegend, San Diego, CA, USA; 1:250 dilution) and Hoechst 33342 (1 µg/mL) for 30 min in the dark. After three washes, images

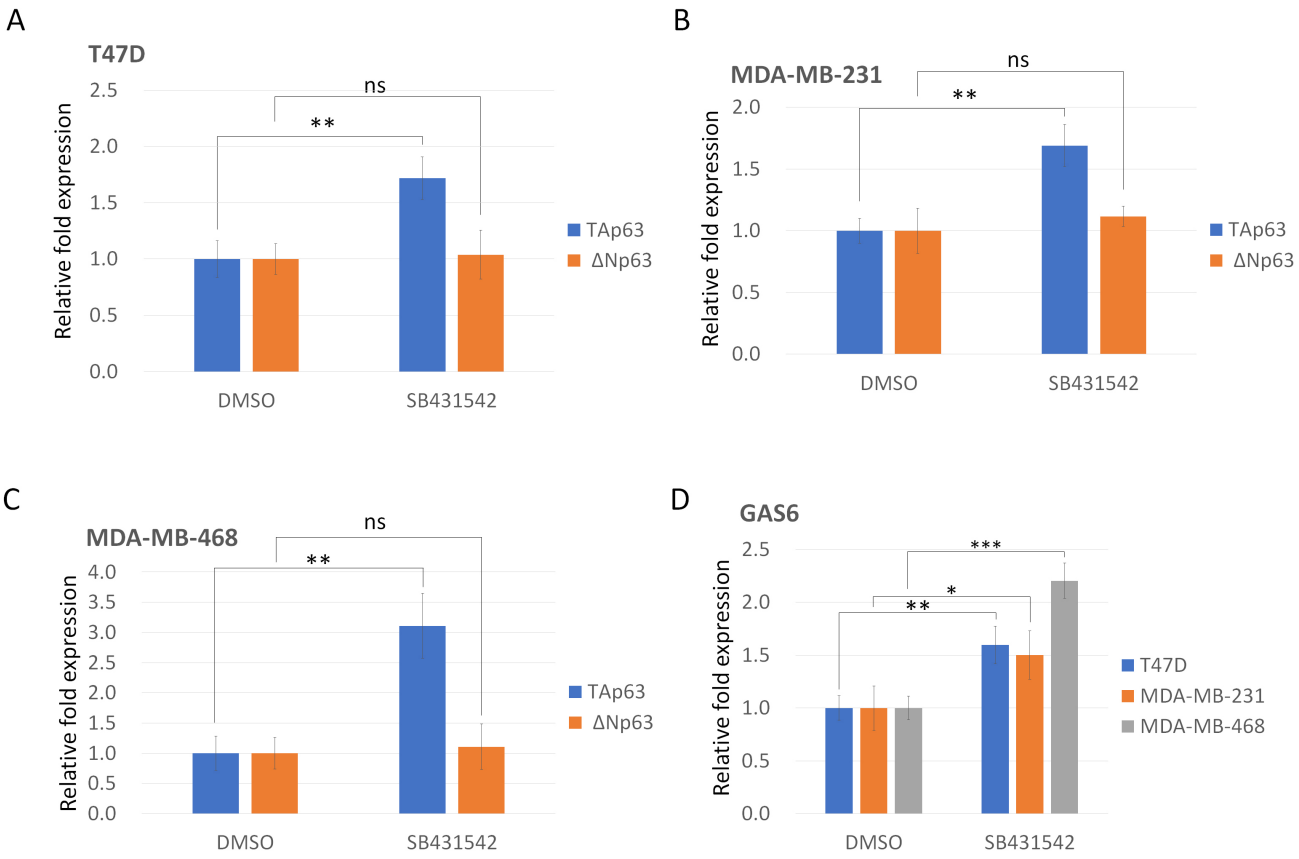

Fig. 1. SB431542 increases TAp63 and its downstream target gene GAS6 expression in p53-mutant breast cancer cells. Breast cancer cells were treated with SB431542 (20 µM) for 48 hours, after which cells were harvested for RNA isolation and analyzed for mRNA expression using quantitative real-time RT-PCR. (A) In T47D cells (harboring the p53 L194F mutation), isoform-specific primers were used to detect the expression of TAp63 and ΔNp63. The results showed that SB431542 treatment led to an increase in TAp63 expression, while ΔNp63 levels remained unchanged. Cells treated with DMSO alone were used as the baseline control and defined as 1, serving as the reference point for normalizing responses to the SB431542 treatment condition. Data are presented as the mean ± standard deviation (SD) from three independent experiments (n = 3) (**, $p < 0.01$; ns, $p > 0.05$). (B) In MDA-MB-231 cells (harboring the p53 R280K mutation), isoform-specific primers were used to examine TAp63 and ΔNp63 expression. SB431542 treatment significantly increased TAp63 expression, with no effect on ΔNp63 expression. Data are presented as the mean ± standard deviation (SD) from three independent experiments (n = 3) (**, $p < 0.01$; ns, $p > 0.05$). (C) In MDA-MB-468 cells (harboring the p53 R273H mutation), isoform-specific primers were employed to detect TAp63 and ΔNp63 expression. The results indicated that SB431542 induced upregulation of TAp63, while ΔNp63 expression remained unaffected. Data are presented as the mean ± standard deviation (SD) from three independent experiments (n = 3) (**, $p < 0.01$; ns, $p > 0.05$). (D) GAS6, a downstream target of p63, was upregulated by SB431542 treatment in all three p53-mutant breast cancer cell lines (T47D, MDA-MB-231, and MDA-MB-468), indicating activation of the p63 signaling pathway. Data are presented as the mean ± standard deviation (SD) from three independent experiments (n = 3) (*, $p < 0.05$; **, $p < 0.01$; ***, $p < 0.001$).

were acquired using an ECLIPSE Ts2 fluorescence microscope (Nikon, Tokyo, Japan). The Mean Gray Value was used to quantify the fluorescence intensity using ImageJ (version 1.53p; National Institutes of Health, Bethesda, MD, USA). [23].

2.6 Activated Caspase-3/7 Detection

Caspase-3/7 activity was measured using the CellEvent Caspase-3/7 Red Detection Reagent (Invitrogen). The reagent was diluted in PBS to a final concentration of 5 µM and added to cells (100 µL per well) after removal of culture medium. Cells were incubated at 37 °C for 30 min in the dark. Nuclei were counterstained with Hoechst 33342 (1 µg/mL). Fluorescent images were captured using an ECLIPSE Ts2 fluorescence microscope (Nikon).

2.7 siRNA Transfection

Cells cultured in 6-well plates were transfected with 25 nM (final concentration) of either control siRNA (sc-

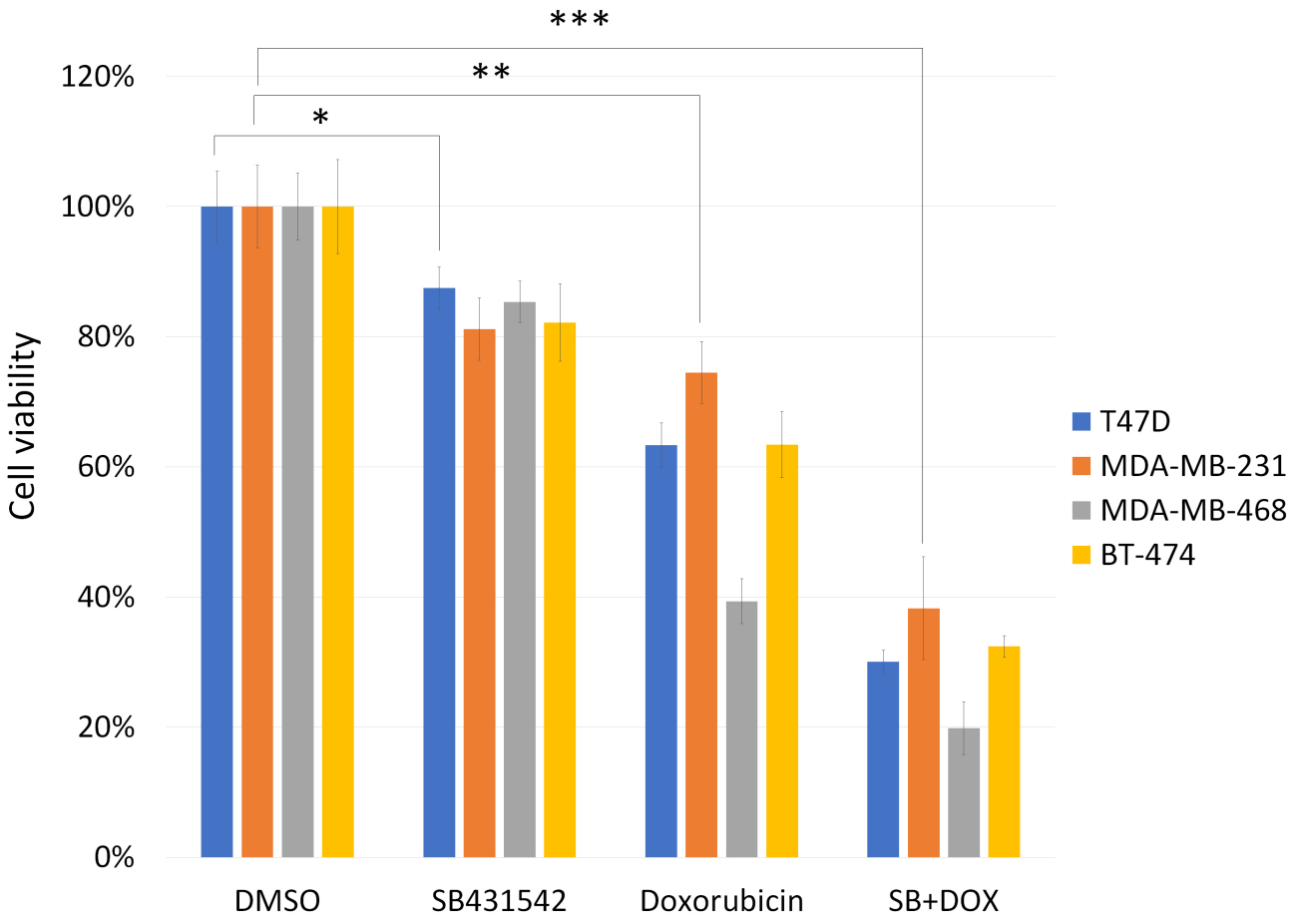

Fig. 2. Cytotoxic effects of SB431542, doxorubicin, or a combination of both on p53-mutated breast cancer cells. T47D, MDA-MB-231, MDA-MB-468 and BT474 breast cancer cells were treated with SB431542 (20 µM), doxorubicin (1 µM), or a combination of both for 48 hours. Cell viability was assessed using the CCK-8 assay. The combination treatment significantly reduced cell viability compared to either agent alone, indicating enhanced cytotoxicity. Cells treated with DMSO alone were used as the baseline control and defined as 100% viability, serving as the reference point for normalizing responses to other drug treatment conditions. Data are presented as the mean ± standard deviation (SD) from three independent experiments (n = 3) (*, $p < 0.05$; **, $p < 0.01$; ***, $p < 0.001$).

37007) or p63 siRNA (sc-36161) using 7.5 µL of TransIT-X2 Transfection Reagent (Mirus Bio, Madison, WI, USA; #MIR6000) for 48 hours. Following transfection, cells were harvested for RNA isolation and subsequently analyzed for p63 expression using quantitative real-time RT-PCR.

2.8 Statistical Analysis

Data are presented as mean ± standard deviation (SD). Comparisons between two groups were performed using a two-tailed Student's *t*-test. A p value of less than 0.05 was considered statistically significant. Significance levels were denoted as: *, $p < 0.05$; **, $p < 0.01$; ***, $p < 0.001$.

3. Results

3.1 SB431542 Induces TAp63 Expression and Upregulates GAS6 in p53-Mutant Breast Cancer Cells

To investigate the effect of SB431542 on the expression of p63 isoforms in p53-mutant breast cancer cells, isoform-specific RT-PCR was performed. In T47D cells harboring the p53 L194F mutation, SB431542 treatment selectively increased TAp63 expression without affecting ΔNp63 levels (Fig. 1A). Similarly, in MDA-MB-231 (p53 R280K) and MDA-MB-468 (p53 R273H) cells, SB431542 significantly induced TAp63 expression, while ΔNp63 remained unchanged (Fig. 1B,C). GAS6, a downstream target of TAp63 [24,25], was upregulated in all three cell lines after SB431542 treatment (Fig. 1D), indicating that the TAp63 transcriptional program was functionally activated.

3.2 SB431542 Enhances the Cytotoxicity of Doxorubicin in p53-Mutant Breast Cancer Cells

We first evaluated a range of SB431542 concentrations in T47D cells while co-treating with a fixed dose of doxorubicin to assess their combined cytotoxic effects (**Supplementary Fig. 1**). From this dose–response analysis, we determined that SB431542 had an IC_{50} value of 37.1 µM under these conditions (**Supplementary Fig. 2**).

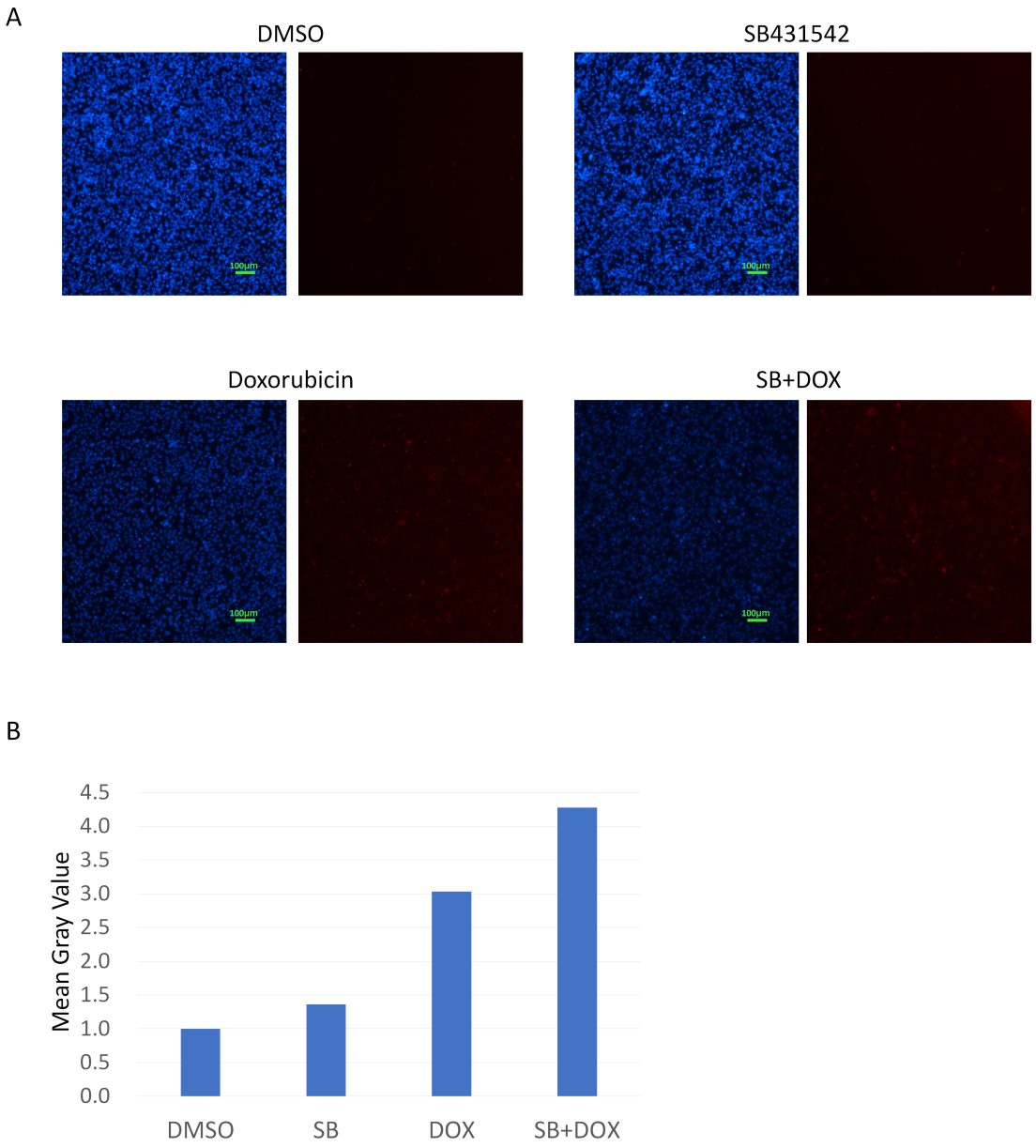

Fig. 3. Caspase-3/7 activation in MDA-MB-231 cells treated with SB431542, doxorubicin, or a combination of both. (A) MDA-MB-231 cells were treated with SB431542, doxorubicin, or a combination of both, followed by direct staining for Caspase-3/7 activity (red fluorescence). Compared to the DMSO control, SB431542 alone caused a slight increase in Caspase-3/7 activation. Doxorubicin alone induced a marked increase in Caspase-3/7 activity. The combination of SB431542 and doxorubicin further enhanced this activation, suggesting a synergistic induction of apoptosis. Hoechst 33342 was used as a nuclear counterstain (blue). Scale bar, 100 µm (10× magnification). (B) Caspase-3/7 fluorescence intensity is dramatically induced by SB431542 and doxorubicin co-treatment. The normalized fluorescence intensity was calculated as the ratio of the red-channel Mean Gray Value to the blue-channel Mean Gray Value, with the DMSO-treated group set to 1.

Notably, among the various concentration combinations, treatment with SB431542 at 20 µM together with doxorubicin at 1 µM resulted in the most pronounced synergistic reduction in cell viability (**Supplementary Table 1**). To determine whether SB431542 sensitizes p53-mutant cells to chemotherapy, T47D, MDA-MB-231, MDA-MB-468, and BT-474 (harboring the p53 E285K mutation) cells were treated with SB431542 (20 µM), doxorubicin (1 µM), or their combination for 48 hours. Cell viability was assessed using the CCK-8 assay (Fig. 2). In all four cell lines, the combination of SB431542 and doxorubicin significantly reduced cell viability compared to either agent alone, indicating a synergistic cytotoxic effect.

Drug interactions were quantitatively evaluated by calculating the Coefficient of Drug Interaction (CDI). CDI values of 0.54 in T47D cells, 0.63 in MDA-MB-231 cells,

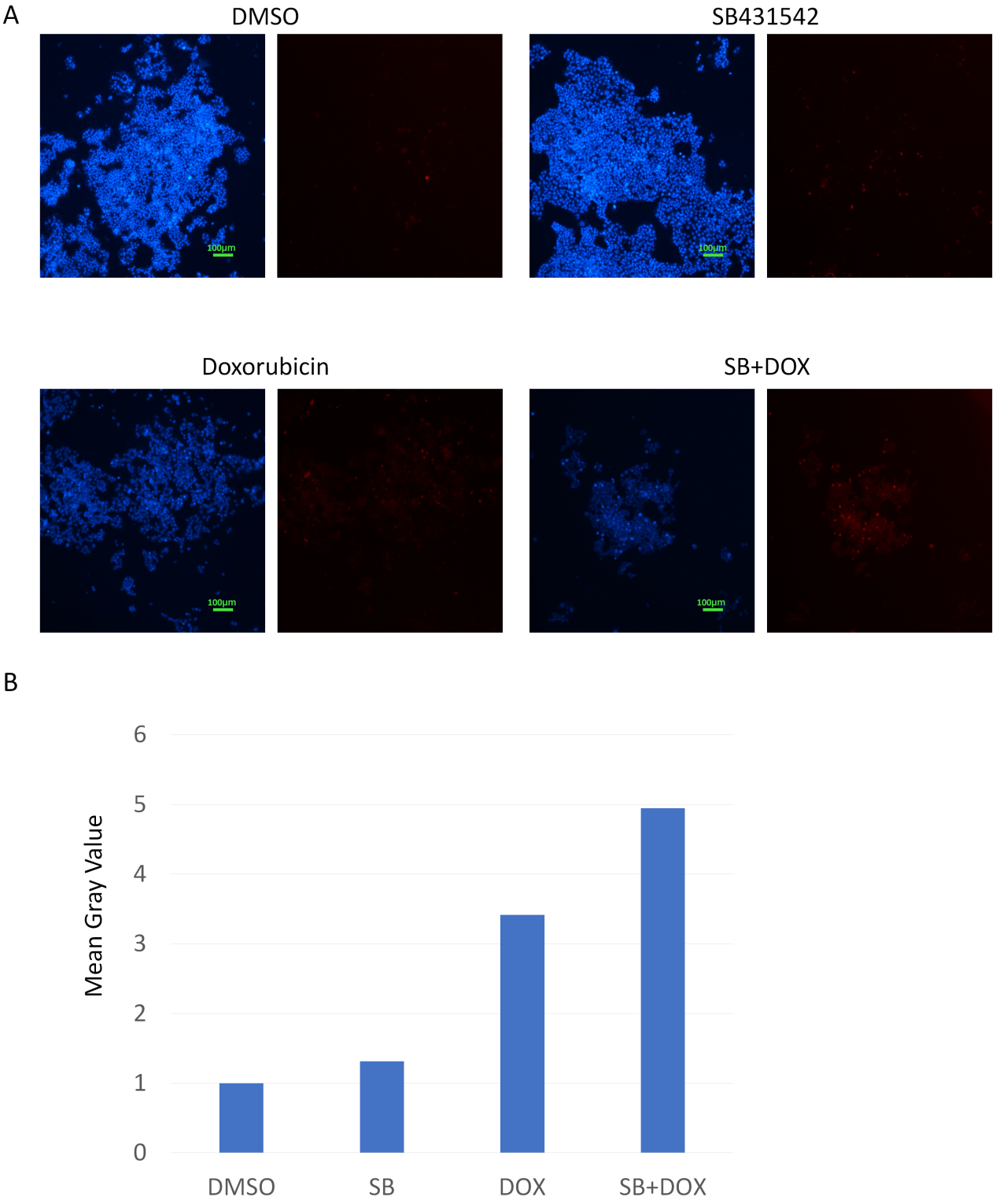

Fig. 4. Caspase-3/7 activation in T47D cells treated with SB431542, doxorubicin, or a combination of both. (A) T47D cells were treated and stained for Caspase-3/7 activity. SB431542 alone resulted in a moderate increase in caspase activation. Doxorubicin significantly induced Caspase-3/7 activity (red). The combination treatment further enhanced both the number and intensity of red fluorescent signals, indicating pronounced apoptotic induction. Hoechst 33342 was used as a nuclear counterstain (blue). Scale bar, 100 μm (10× magnification). (B) SB431542 and doxorubicin co-treatment markedly enhanced Caspase-3/7 fluorescence. Intensity was normalized by the red-to-blue Mean Gray Value ratio, using DMSO as the reference (set to 1).

Table 1. Calculation of the coefficient of drug interaction (CDI) in p53-mutated breast cancer cells treated with SB431542 and doxorubicin.

Table 1A

	DMSO	SB431542 20 µM	Doxorubicin 1 µM	SB+DOX
T47D	100.00 (%)	87.45 (%)	63.32 (%)	30.03 (%)
CDI = [survival% (Drug A + DrugB)] / [survival% (Drug A) * survival% (Drug B)]				CDI 0.54

Table 1B

	DMSO	SB431542 20 µM	Doxorubicin 1 µM	SB+DOX
MDA-MB-231	100.00 (%)	81.14 (%)	74.51 (%)	38.27 (%)
CDI = [survival% (Drug A + DrugB)] / [survival% (Drug A) * survival% (Drug B)]				CDI 0.63

Table 1C

	DMSO	SB431542 20 µM	Doxorubicin 1 µM	SB+DOX
MDA-MB-468	100.00 (%)	85.36 (%)	39.36 (%)	19.87 (%)
CDI = [survival% (Drug A + DrugB)] / [survival% (Drug A) * survival% (Drug B)]				CDI 0.59

Table 1D

	DMSO	SB431542 20 µM	Doxorubicin 1 µM	SB+DOX
BT-474	100.00 (%)	82.15 (%)	63.39 (%)	32.40 (%)
CDI = [survival% (Drug A + DrugB)] / [survival% (Drug A) * survival% (Drug B)]				CDI 0.62

The drug interaction between SB431542 and doxorubicin was evaluated using the Coefficient of Drug Interaction (CDI), calculated as: CDI = AB/(A × B), where AB is the relative viability (%) of the combination treatment, and A and B are the relative viabilities (%) of each single-agent treatment. (A) In T47D cells, the CCK-8 assay (Fig. 2) yielded a CDI of 0.54, indicating a synergistic (additive cytotoxic) effect. (B) In MDA-MB-231 cells, the calculated CDI was 0.63, also indicating a synergistic (additive cytotoxic) effect. (C) In MDA-MB-468 cells, the CDI was 0.59, again indicating a synergistic (additive cytotoxic) effect. (D) In BT-474 cells, the CDI was 0.62, again indicating a synergistic (additive cytotoxic) effect.

0.59 in MDA-MB-468 cells, and 0.62 in BT-474 (Table 1) all fell below 1, further confirming a synergistic interaction between SB431542 and doxorubicin.

3.3 Combination Treatment Synergistically Activates Caspase-3/7

To assess apoptosis induction, caspase-3/7 activity was examined by fluorescent staining. In MDA-MB-231 cells, SB431542 induced a mild increase in caspase-3/7 activation, whereas doxorubicin caused a more substantial effect. The combination treatment led to a pronounced increase in red fluorescence, indicating enhanced apoptotic signaling (Fig. 3). Similarly, in T47D cells, SB431542 alone modestly increased caspase activity, whereas doxorubicin induced a strong response. The combination further amplified both the intensity and frequency of caspase-positive cells (Fig. 4), consistent with a synergistic apoptotic effect.

3.4 p63 Expression is Elevated by SB431542 and Doxorubicin, and Correlates With Apoptotic Induction

Immunofluorescence staining revealed cell line-specific effects on p63 protein expression. In MDA-MB-231 cells, SB431542 alone had minimal impact on p63 levels, while doxorubicin induced a clear upregulation. The combination treatment further increased the proportion of p63-positive nuclei, despite a reduction in overall cell number (Fig. 5). In T47D cells, SB431542 alone significantly elevated p63 expression, which was further enhanced by doxorubicin (Fig. 6). SB431542 and doxorubicin elicited

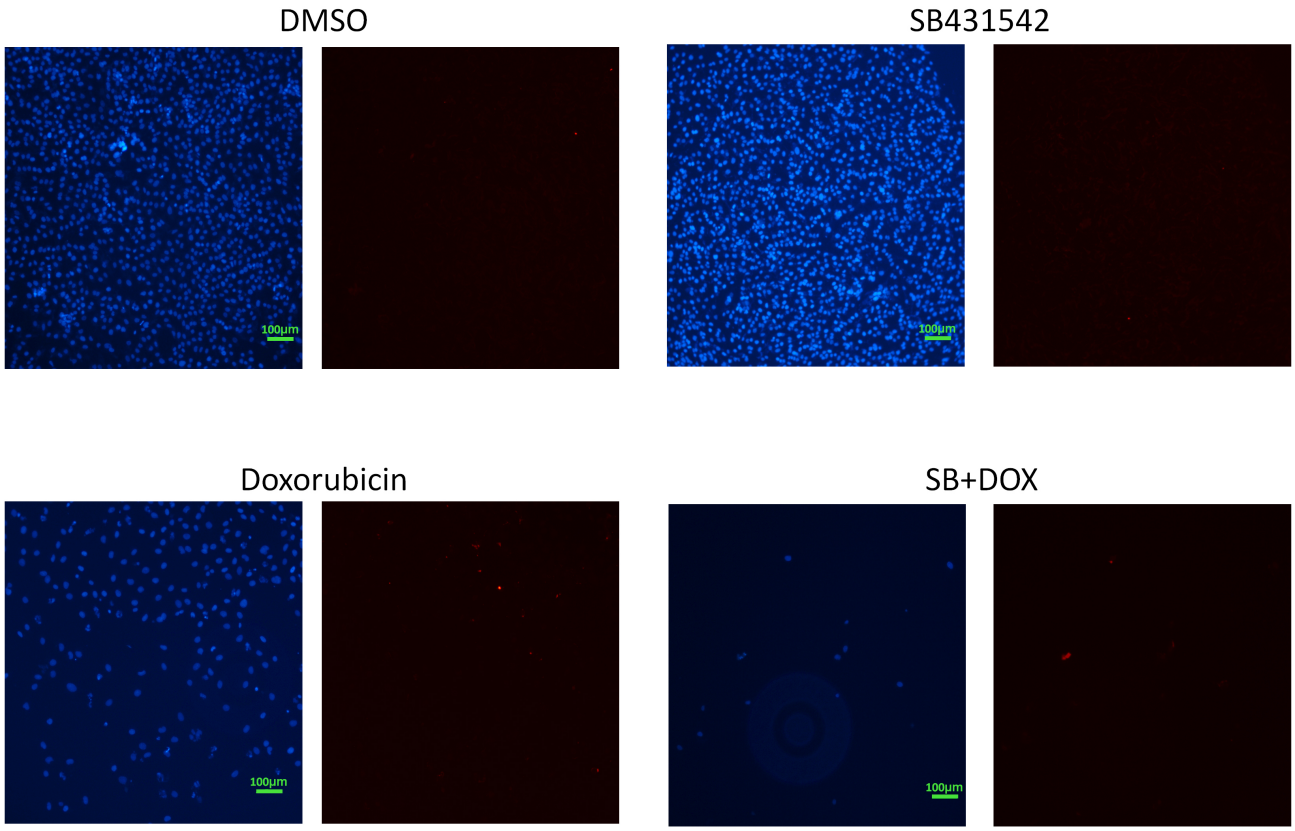

Fig. 5. p63 expression in MDA-MB-231 cells detected by immunofluorescence. MDA-MB-231 cells were stained for p63 (red). SB431542 treatment did not markedly alter p63 levels. In contrast, doxorubicin increased p63 expression. Combination treatment with SB431542 and doxorubicin, although reducing overall cell number, resulted in a nearly 1:1 ratio of red fluorescent signals to nuclei, indicating an increased p63 expression per cell. Hoechst 33342 was used as a nuclear counterstain (blue). Scale bar, 100 µm (10×).

comparable p63 induction in MDA-MB-468 and BT-474 cells (**Supplementary Figs. 3,4**). Notably, nearly all surviving cells exhibited strong nuclear p63 signals under combination treatment, suggesting a link between p63 activation and apoptosis (Figs. 5,6, **Supplementary Figs. 3,4**).

3.5 Cytotoxicity Induced by SB431542 and Doxorubicin Requires p53 Family and Caspase Activity

To determine whether the cytotoxic effect of the combination treatment is dependent on p53 family signaling, breast cancer cells were treated with SB431542 and doxorubicin in the presence or absence of PETα, a pan-inhibitor of p53 family transcriptional activity [26–28]. Co-treatment with PETα significantly rescued cell viability (Fig. 7), indicating that p53 family members, likely TAp63, mediate the observed cytotoxicity.

Furthermore, the pan-caspase inhibitor (Z-VAD-FMK) reversed the reduction in cell viability caused by the combination treatment (Fig. 8), demonstrating that caspase activity is required for the observed cell death, and confirming the apoptotic nature of the cytotoxic response.

3.6 Cytotoxicity of SB431542 and Doxorubicin is Mediated by p63

To determine whether p63 mediates the cytotoxic effects of SB431542 and doxorubicin, we performed p63 knockdown using siRNA. Both SB431542 and doxorubicin induced TAp63 expression, and this induction was abolished by p63 siRNA (Fig. 9A). The combination of SB431542 and doxorubicin further enhanced p63 expression, which was likewise reversed by p63 knockdown. Consistently, treatment with SB431542, doxorubicin, or a combination of both significantly reduced cell viability; however, these cytotoxic effects were markedly rescued in cells transfected with p63 siRNA (Fig. 9B). These findings indicate that p63 plays a critical role in mediating the cytotoxicity induced by SB431542 and doxorubicin.

3.7 p63 Shows Significant Differential Expression in Breast Cancer and Influences Patient Survival

To further investigate the role of p63 in breast cancer, we analyzed its expression across cancer types and clinical subgroups. According to the UALCAN database [29], the most pronounced reduction in p63 expression occurs specifically in breast cancer and prostate adenocarcinoma, a pattern not observed in most other cancer types

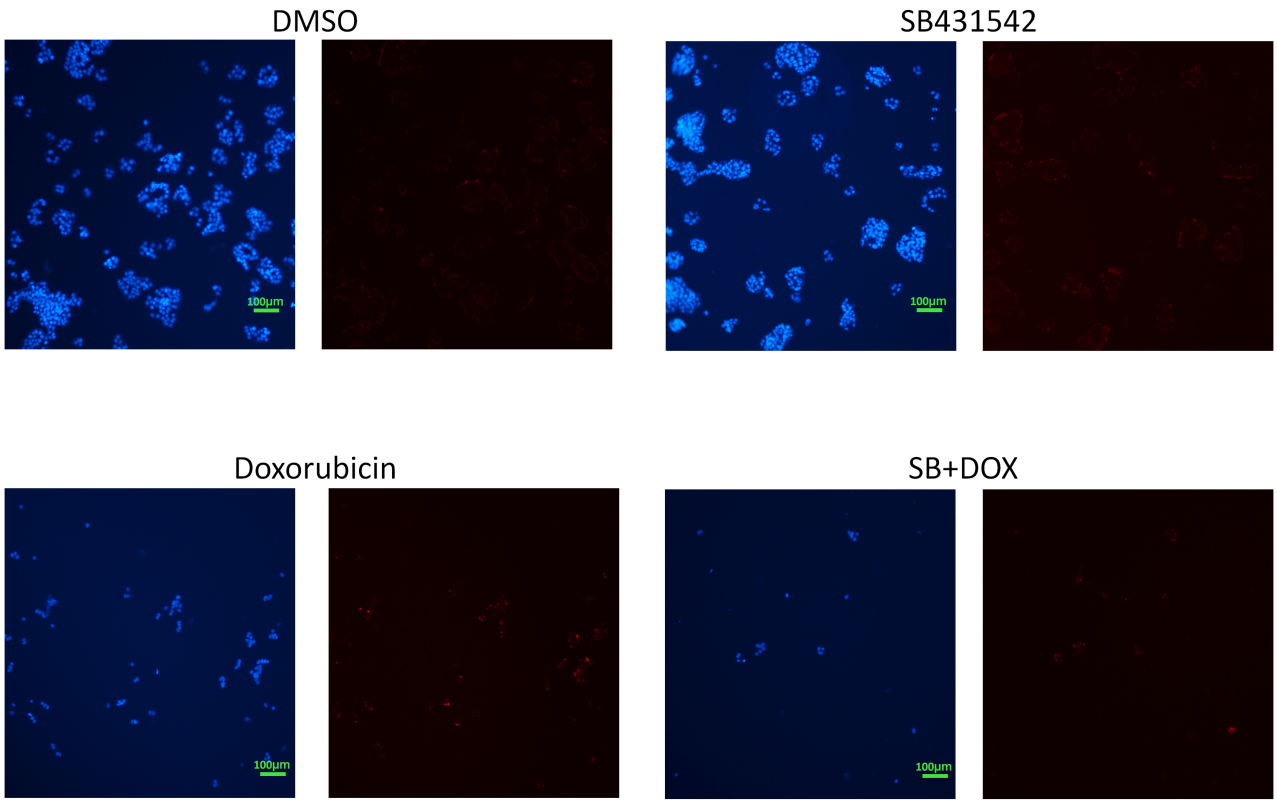

Fig. 6. p63 expression in T47D cells detected by immunofluorescence. T47D cells showed a substantial increase in p63 expression (red) upon treatment with SB431542 alone. Doxorubicin similarly induced p63 expression. The combination treatment resulted in a reduced number of cells, but with nearly all nuclei showing p63 positivity, further confirming increased p63 expression and suggesting a link to apoptotic activity. Hoechst 33342 was used as a nuclear counterstain (blue). Scale bar, 100 µm (10×).

(Fig. 10A). Consistent with this finding, p63 expression was markedly lower in breast cancer tissue compared with normal breast tissue (Fig. 10B). Within breast cancer subtypes, p63 expression follows the trend: normal > luminal > HER2-positive > triple-negative breast cancer (TNBC) (Fig. 10C). When considering disease stage, stage IV tumors show substantially lower p63 levels compared with stages I–III (Fig. 10D). Furthermore, tumors harboring p53 mutations exhibit significantly reduced p63 expression relative to p53 wild-type tumors (Fig. 10E). Because HER2-positive and TNBC groups included too few cases with high p63 expression, meaningful survival analysis was only feasible for the luminal subtype. In this group, patients with high p63 expression consistently demonstrated better survival at 1000–3000 days compared with those with low p63 expression (Fig. 10F).

4. Discussion

Our findings demonstrate that SB431542 enhances the cytotoxic and apoptotic effects of doxorubicin in breast cancer cells harboring mutant p53, particularly through mechanisms involving TAp63 activation. In p53-mutated breast cancer cells, combination treatment with SB431542 and doxorubicin significantly reduced cell viability, as evidenced by CCK-8 assay results (Fig. 2), and yielded a CDI value of 0.54–0.63 (Table 1), indicating a synergistic interaction. Apoptosis was markedly increased in both MDA-MB-231 and T47D cells upon combination treatment, as indicated by enhanced caspase-3/7 activity (Figs. 3,4). These results are consistent with prior reports that TGF-β pathway inhibition can sensitize cancer cells to chemotherapeutic agents by enhancing apoptotic signaling [30].

Mechanistically, our data suggest that the enhanced apoptosis induced by SB431542 and doxorubicin is at least partially mediated through the activation of p63. Immunofluorescence staining revealed that p63 expression was upregulated in T47D and MDA-MB-231 cells treated with either SB431542 or doxorubicin, with further enhancement observed upon combination treatment (Figs. 5,6). Since TAp63 has been shown to promote apoptosis, cell cycle arrest, and DNA damage response in p53-deficient contexts [16,31], these findings support the hypothesis that SB431542 may enhance doxorubicin-induced cytotoxicity by upregulating TAp63. This is further supported by the reversal of cytotoxicity upon co-treatment with PETα, a p53 family inhibitor (Fig. 7), implicating the p53 family, likely TAp63, as a key mediator of the observed antitumor effects.

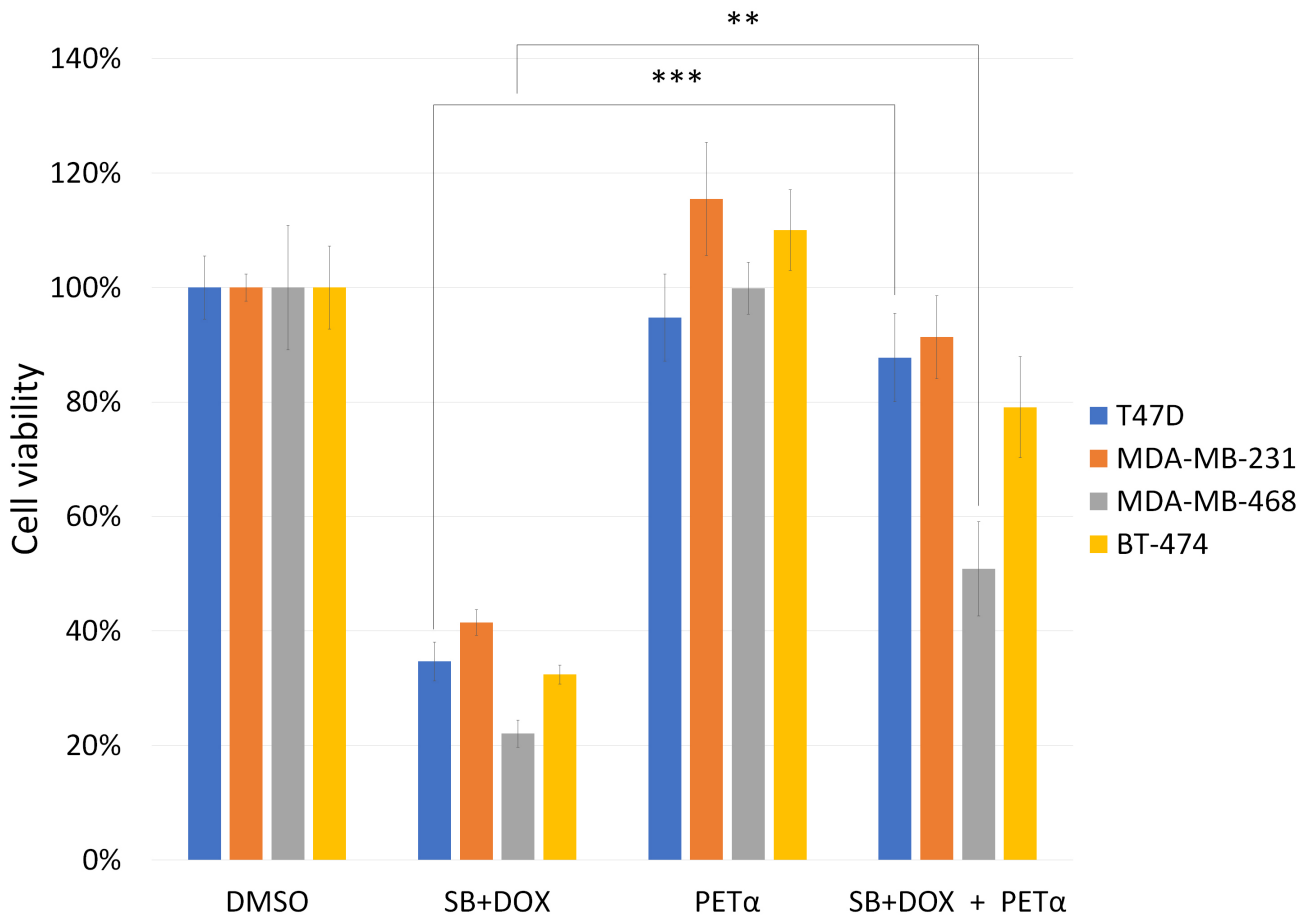

Fig. 7. Effect of p53 family inhibition on SB431542 and doxorubicin cytotoxicity in breast cancer cells. T47D, MDA-MB-231, MDA-MB-468 and BT-474 cells were treated with SB431542, doxorubicin, and a combination of both with or without the p53 family inhibitor PETα. Cell viability was assessed after 48 hours using a CCK-8 assay. The combination of SB431542 and doxorubicin significantly reduced cell viability. This cytotoxic effect was reversed upon co-treatment with PETα, suggesting that the observed cytotoxicity is dependent on p53 family signaling. Cells treated with DMSO alone served as the baseline control and were designated as having 100% viability, providing the reference for normalizing responses to other drug treatments. Data are expressed as the mean $\pm$ standard deviation (SD) from three independent experiments (n = 3). Statistical significance is indicated as follows: **, $p < 0.01$; ***, $p < 0.001$.

Our results also indicate that apoptosis is the primary mode of cell death induced by the combination treatment, as evidenced by caspase dependency. Co-treatment with a pan-caspase inhibitor (Z-VAD-FMK) significantly attenuated the cytotoxic effect of SB431542 and doxorubicin in both T47D and MDA-MB-468 cells (Fig. 8), consistent with caspase-3/7 activation data. This suggests that the observed cell death is caspase-mediated and apoptotic in nature. Previous studies have demonstrated that activation of TAp63 can trigger mitochondrial apoptosis pathways, particularly in the context of p53 mutation or loss [16]. Our findings align with these observations and extend them by identifying a novel combination—SB431542 plus doxorubicin—that effectively activates this alternative apoptotic pathway in mutant p53 breast cancer models.

This research provides compelling evidence that SB431542 enhances the antitumor efficacy of doxorubicin in breast cancer cells with mutant p53, through a mechanism that involves activation of TAp63 and caspase-mediated apoptosis. This is of clinical interest as TP53 mutations are present in over 30% of breast cancers, particularly in aggressive subtypes such as triple-negative breast cancer (TNBC), and are often associated with poor response to chemotherapy and increased recurrence [32]. Targeting the function of mutant p53 may pave the way for novel treatments in aggressive TNBC [33]. In this study, two cell lines—MDA-MB-231, and MDA-MB-468—were TNBC cells. This means our findings are particularly relevant to TNBC, a breast cancer subtype that currently lacks targeted therapies and is often resistant to conventional chemotherapy. The observed enhancement of doxorubicin efficacy by SB431542 suggests that this combination could represent a promising therapeutic strategy specifically for TNBC patients harboring TP53 mutations. By activating alternative

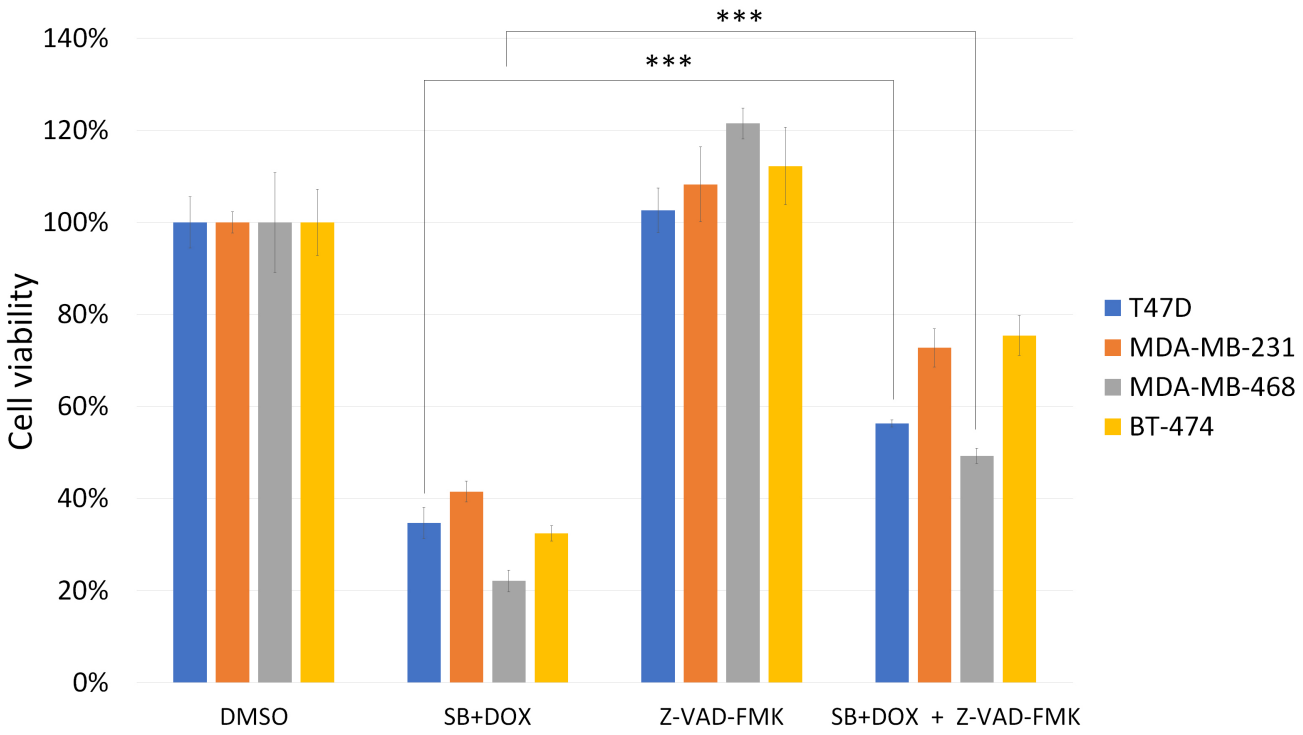

Fig. 8. Effect of caspase inhibition on SB431542 and doxorubicin cytotoxicity in breast cancer cells. T47D, MDA-MB-231, MDA-MB-468 and BT-474 cells were treated as above, with or without the pan-caspase inhibitor (Z-VAD-FMK). Similar to Fig. 7, the combination of SB431542 and doxorubicin significantly reduced cell viability after 48 hours. Co-treatment with Z-VAD-FMK reversed this effect, indicating that the cell death induced by SB431542 and doxorubicin is caspase-dependent and likely apoptotic in nature. Cells treated with DMSO alone were used as a 100% viability control, serving as the reference for normalizing responses to drug treatments. Data are presented as mean ± standard deviation (SD) from three independent experiments (n = 3). Statistical significance is indicated as follows: ***, $p < 0.001$.

tumor-suppressive pathways such as TAp63 and promoting caspase-mediated apoptosis, this approach may help overcome the limitations imposed by mutant p53 and improve clinical outcomes in this challenging breast cancer subtype.

A key mechanistic insight from our work is the observed upregulation of p63 expression, both at baseline in SB431542-treated cells and in combination with doxorubicin (Figs. 5,6). TAp63, a structural homolog of p53, has been shown to compensate for p53 loss by activating similar downstream pro-apoptotic targets such as BAX, PUMA, and NOXA [34,35]. The reversal of cytotoxicity upon treatment with the p53 family inhibitor PETα (Fig. 7) further confirms the central role of p63 in mediating this chemosensitizing effect. Given that doxorubicin also induces p63 expression, it is plausible that SB431542 acts as a TAp63 amplifier, enabling more robust transcriptional activation of apoptotic genes.

T47D (harboring the p53 L194F mutation) and MDA-MB-231 (with the p53 R280K mutation) breast cancer cell lines carry aggregated forms of p53 mutations [36]. Both cell lines exhibited higher resistance to the chemotherapeutic drug doxorubicin than MDA-MB-468 cells, which carry the non-aggregated p53 R273H mutation and demonstrated a better response to doxorubicin [37]. Our combination treatment produced significantly synergistic effects in all three cell lines, as indicated by coefficient of drug interaction (CDI) values below 0.7. This suggests a synergistic interaction regardless of the p53 mutation aggregation status. Therefore, this drug pairing shows potential therapeutic benefit in breast cancers with either aggregated or non-aggregated types of p53 mutations.

In addition, emerging evidence suggests that TGF-β pathway inhibition may also indirectly modulate the tumor immune microenvironment. Although our current in vitro data do not directly address immune interactions, the TGF-β blocking antibody or SB431542 has been reported to enhance anti-tumor immunity *in vivo* by reducing immunosuppressive signaling and promoting cytotoxic T-cell activity [38–40]. Therefore, combining SB431542 with doxorubicin may yield both direct cytotoxic effects and immunomodulatory benefits, which could be further explored in immunocompetent animal models.

Further analysis shows that p63 expression is consistently and markedly reduced in breast cancer compared with normal tissue (Fig. 10B). Interestingly, this pronounced downregulation was highly cancer-type specific, occurring

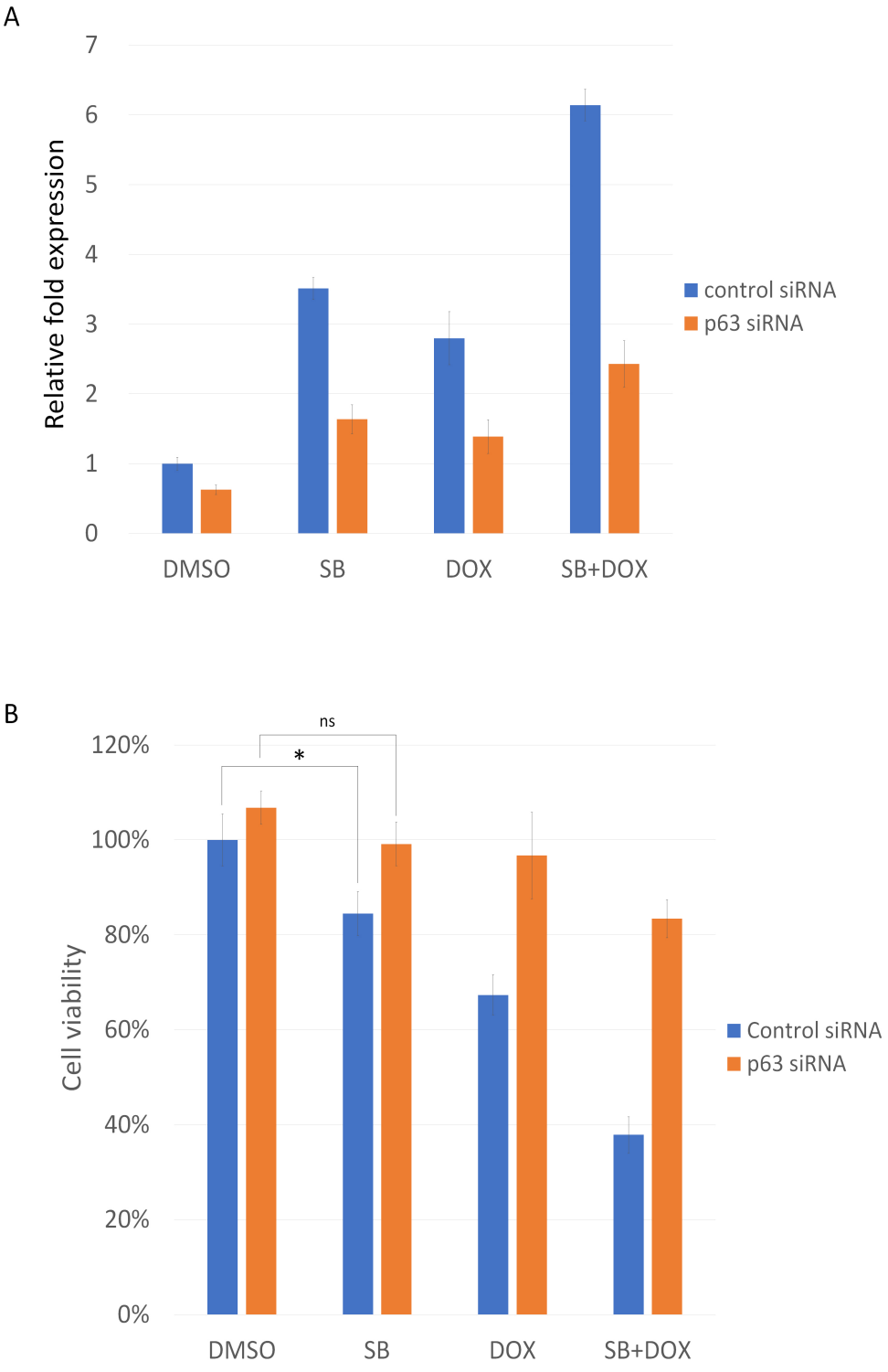

Fig. 9. p63 mediates the cytotoxic effects of SB431542 and doxorubicin. (A) Real-Time RT-PCR analysis showing TAp63 expression following treatment with SB431542, doxorubicin, or a combination of both, with or without p63 siRNA. Drug-induced TAp63 upregulation is reversed by p63 knockdown. Cells transfected with control siRNA and subsequently treated with DMSO alone were used as the baseline control and set to a relative value of 1. (B) Cell viability assays demonstrating reduced viability after SB431542, doxorubicin, or combination treatment. The decrease in viability is rescued by p63 knockdown, indicating p63-dependent cytotoxicity. Cells transfected with control siRNA and subsequently treated with DMSO alone served as the baseline control and were designated as 100% viable. Data are presented as the mean ± standard deviation (SD) from three independent experiments (n = 3) (*, $p < 0.05$; ns, $p > 0.05$).

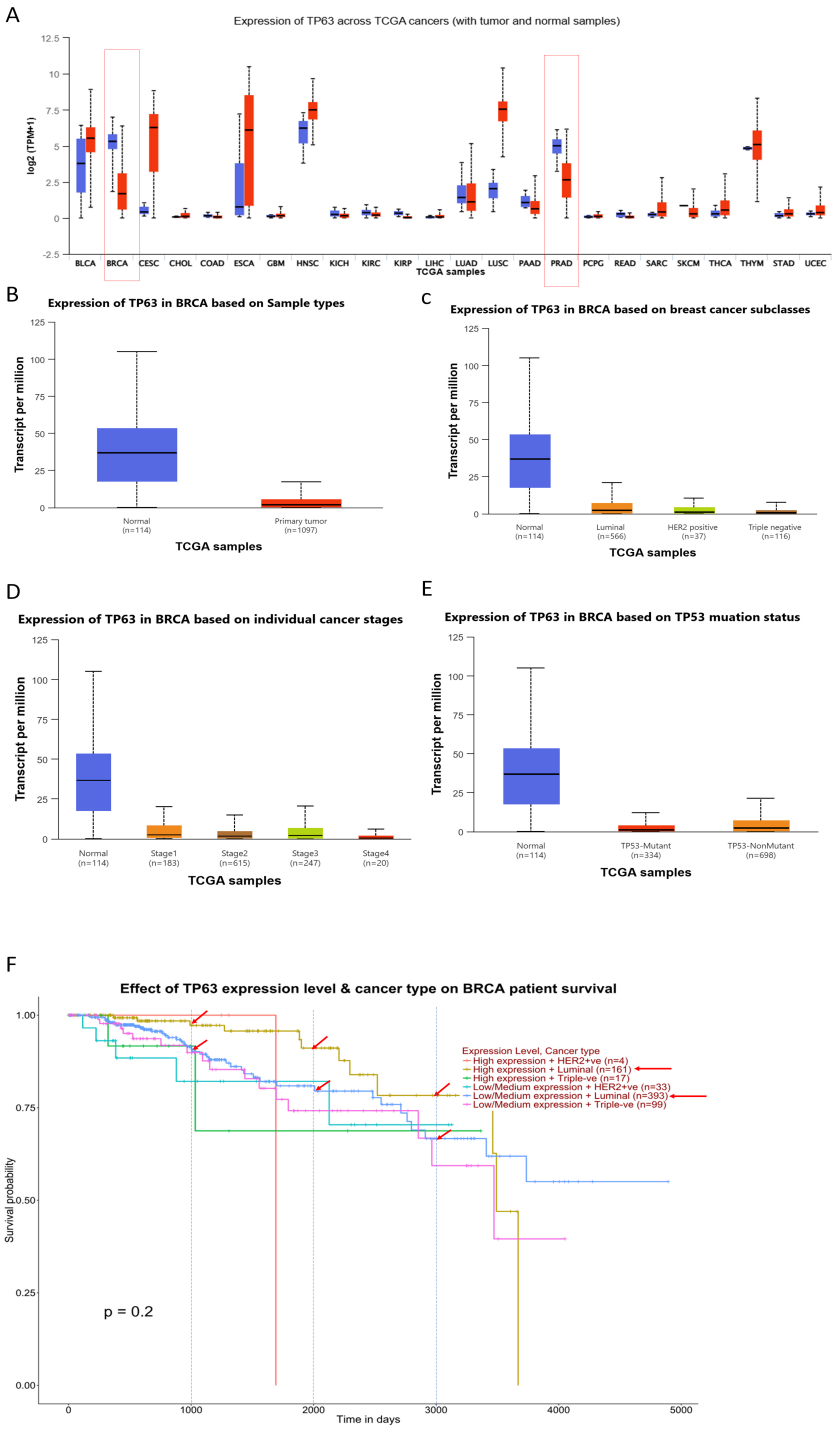

Fig. 10. p63 expression patterns and clinical significance in breast cancer. (A) Pan-cancer analysis of p63 expression across multiple tumor types. A marked downregulation of p63 is observed specifically in breast cancer and prostate adenocarcinoma (red columns), whereas most other cancers do not show significant changes. (B) Comparison of p63 expression between normal breast tissue and breast cancer samples. Breast cancer shows significantly reduced p63 expression. (C) p63 expression across breast cancer subtypes. Expression levels follow the trend: normal > luminal > HER2-positive > triple-negative breast cancer (TNBC). (D) p63 expression according to clinical stage. Stage IV tumors exhibit substantially lower p63 expression compared with stages I–III. (E) Relationship between p63 expression and p53 mutation status. Tumors with p53 mutations display significantly lower p63 levels than p53 wild-type tumors. (F) Kaplan–Meier survival analysis of luminal breast cancer patients stratified by p63 expression shows that high p63 levels are associated with improved overall survival at 1000, 2000, and 3000 days (red arrows). HER2-positive and TNBC subtypes were not further evaluated due to the limited number of patients with high p63 expression.

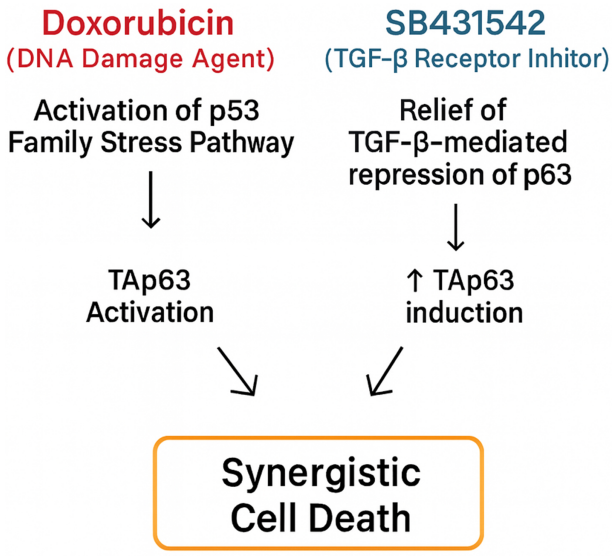

Fig. 11. Proposed mechanism underlying the synergistic effects of SB431542 and doxorubicin via convergent activation of the p63-dependent apoptotic pathway. Doxorubicin induces DNA damage, leading to activation of p53-family stress signaling and activation of TAp63. Concurrently, SB431542 inhibits TGF-β/SMAD signaling, relieving TGF-β–mediated repression of p63 and its downstream pro-apoptotic targets. When combined, the two drugs converge on a common apoptotic axis, leading to amplified TAp63 activation and enhanced expression of apoptotic genes, ultimately driving synergistic cell death.

prominently in breast cancer and prostate adenocarcinoma but not in most other malignant tissues (Fig. 10A), indicating a context-dependent regulatory function.

Within breast cancer, lower p63 expression was strongly associated with more aggressive clinicopathological features, including HER2-positive and triple-negative subtypes (Fig. 10C). These subtypes are characterized by higher proliferative indices and poorer outcomes, suggesting that loss of p63 may contribute to tumor progression or reflect dedifferentiation of epithelial cells. Similarly, the decrease in p63 expression observed in stage IV disease supports the notion that p63 reduction may correlate with metastatic capability or advanced tumor biology (Fig. 10D).

A particularly notable finding is the association between p53 mutation and reduced p63 expression in breast cancer (Fig. 10E). We demonstrated that p63 expression can be successfully restored in TP53-mutant breast cancer cells using SB431542, particularly in combination with doxorubicin. This pharmacologic induction of p63 suggests that, despite the presence of mutant p53, the TAp63 pathway remains responsive to external modulation. The ability of SB431542 plus doxorubicin to elevate p63 levels and reactivate downstream apoptotic signaling highlights a potential therapeutic strategy to counteract the loss of p53 function and improve treatment responsiveness in these otherwise chemoresistant tumors.

Doxorubicin induces DNA damage and activates p53 family stress signaling [16,41], leading to induction of TAp63 activation. In contrast, SB431542 blocks TGF-β/SMAD signaling, which normally suppresses p63 [42, 43]. By relieving this repression, SB431542 enhanced TAp63 expression. When combined, both agents converge on the same p63-dependent apoptotic pathway, amplifying pro-apoptotic gene expression and overcoming compensatory survival mechanisms. As a result, SB431542 and doxorubicin produce a synergistic cytotoxic effect through coordinated activation of TAp63-mediated apoptosis (Fig. 11).

Our findings provide a strong mechanistic rationale for combining the TGF-β inhibitor SB431542 with doxorubicin to treat mutant p53 breast cancer. This approach effectively bypasses the dysfunctional p53 pathway by engaging the TAp63-dependent cell death mechanism. The strategy is highly feasible, supported by the existence of a clinical-grade TGF-β inhibitor (e.g., Galunisertib), which can translate our findings. The current major constraint is the absence of *in vivo* data. Future studies to validate the efficacy and safety of this combination using a clinically relevant TGF-β inhibitor in animal models will be imperative before proceeding to clinical trials

5. Conclusion

Our findings identify a novel drug combination—SB431542 plus doxorubicin—that effectively activates an alternative apoptotic pathway in mutant p53 breast cancer models. Our findings highlight a previously underexplored therapeutic strategy: targeting the TGF-β/TAp63 axis to restore apoptosis in mutant p53 cancers. This approach may be particularly effective in tumors with compromised p53 function and resistance to conventional chemotherapeutics. Future studies will focus on validating this strategy in vivo, exploring combination regimens with immune checkpoint inhibitors, and identifying predictive biomarkers of TAp63 responsiveness to guide patient selection.

Availability of Data and Materials

The data are available from the corresponding authors on reasonable request.

Author Contributions

YLK, CCC and BHC conceived and designed the study. YLK, YJL, TCH, KYW and STC performed experiments. JYC, KYL, HHW and YTC performed the statistical analysis. CCC and BHC received fundings to support research. BHC wrote the manuscript. CCC and BHC conducted review and editing. All authors contributed to editorial changes in the manuscript. All authors read and approved the final manuscript. All authors have participated sufficiently in the work and agreed to be accountable for all aspects of the work.

Ethics Approval and Consent to Participate

Not applicable.

Acknowledgment

We would like to acknowledge the technical support given by the Basic Medical Core Laboratory, I-Shou University College of Medicine.

Funding

This research was supported by the Medical Student Research and Development Scholarship Program [EDAHS112038], and the grant of E-DA Hospital [EDAHJ114001].

Conflict of Interest

The authors declare no conflict of interest.

Supplementary Material

Supplementary material associated with this article can be found, in the online version, at https://doi.org/10.31083/FBL45389.

References

[1] Inman GJ, Nicolás FJ, Callahan JF, Harling JD, Gaster LM, Reith AD, *et al*. SB-431542 is a potent and specific inhibitor of transforming growth factor-beta superfamily type I activin receptor-like kinase (ALK) receptors ALK4, ALK5, and ALK7. Molecular Pharmacology. 2002; 62: 65–74. https://doi.org/10.1124/mol.62.1.65.

[2] Tan F, Qian C, Tang K, Abd-Allah SM, Jing N. Inhibition of transforming growth factor β (TGF-β) signaling can substitute for Oct4 protein in reprogramming and maintain pluripotency. The Journal of Biological Chemistry. 2015; 290: 4500–4511. https://doi.org/10.1074/jbc.M114.609016.

[3] Mahmood A, Harkness L, Schrøder HD, Abdallah BM, Kassem M. Enhanced differentiation of human embryonic stem cells to mesenchymal progenitors by inhibition of TGF-beta/activin/nodal signaling using SB-431542. Journal of Bone and Mineral Research: the Official Journal of the American Society for Bone and Mineral Research. 2010; 25: 1216–1233. https://doi.org/10.1002/jbmr.34.

[4] Halder SK, Beauchamp RD, Datta PK. A specific inhibitor of TGF-beta receptor kinase, SB-431542, as a potent antitumor agent for human cancers. Neoplasia. 2005; 7: 509–521. https://doi.org/10.1593/neo.04640.

[5] Sarkar P, Randall SM, Collier TS, Nero A, Russell TA, Muddiman DC, *et al*. Activin/nodal signaling switches the terminal fate of human embryonic stem cell-derived trophoblasts. The Journal of Biological Chemistry. 2015; 290: 8834–8848. https://doi.org/10.1074/jbc.M114.620641.

[6] Pokorná Z, Tylichová Z, Vojtesek B, Coates PJ. Complex and variable regulation of ΔNp63 and TAp63 by TGFβ has implications for the dynamics of squamous cell epithelial to mesenchymal transition. Scientific Reports. 2024; 14: 7304. https://doi.org/10.1038/s41598-024-57895-1.

[7] Cai BH, Chao CF, Lu MH, Lin HC, Chen JY. A half-site of the p53-binding site on the keratin 14 promoter is specifically activated by p63. Journal of Biochemistry. 2012; 152: 99–110. https://doi.org/10.1093/jb/mvs053.

[8] Yang A, McKeon F. P63 and P73: P53 mimics, menaces and more. Nature Reviews. Molecular Cell Biology. 2000; 1: 199–207. https://doi.org/10.1038/35043127.

[9] Yang A, Kaghad M, Wang Y, Gillett E, Fleming MD, Dötsch V, *et al*. p63, a p53 homolog at 3q27-29, encodes multiple products with transactivating, death-inducing, and dominant-negative activities. Molecular Cell. 1998; 2: 305–316. https://doi.org/10.1016/s1097-2765(00)80275-0.

[10] Cai BH, Chao CF, Huang HC, Lee HY, Kannagi R, Chen JY. Roles of p53 Family Structure and Function in Non-Canonical Response Element Binding and Activation. International Journal of Molecular Sciences. 2019; 20: 3681. https://doi.org/10.3390/ijms20153681.

[11] Napoli M, Li X, Ackerman HD, Deshpande AA, Barannikov I, Pisegna MA, *et al*. Pan-cancer analysis reveals TAp63-regulated oncogenic lncRNAs that promote cancer progression through AKT activation. Nature Communications. 2020; 11: 5156. https://doi.org/10.1038/s41467-020-18973-w.

[12] Guo X, Keyes WM, Papazoglu C, Zuber J, Li W, Lowe SW, *et al*. TAp63 induces senescence and suppresses tumorigenesis in vivo. Nature Cell Biology. 2009; 11: 1451–1457. https://doi.org/10.1038/ncb1988.

[13] Park GB, Jeong JY, Kim D. Gliotoxin Enhances Autophagic Cell Death via the DAPK1-TAp63 Signaling Pathway in Paclitaxel-Resistant Ovarian Cancer Cells. Marine Drugs. 2019; 17: 412. https://doi.org/10.3390/md17070412.

[14] Cai BH, Hsu YC, Yeh FY, Lin YR, Lu RY, Yu SJ, *et al*. P63 and P73 Activation in Cancers with p53 Mutation. Biomedicines. 2022; 10: 1490. https://doi.org/10.3390/biomedicines10071490.

[15] Petitjean A, Cavard C, Shi H, Tribollet V, Hainaut P, Caron de Fromentel C. The expression of TA and DeltaNp63 are regulated by different mechanisms in liver cells. Oncogene. 2005; 24: 512–519. https://doi.org/10.1038/sj.onc.1208215.

[16] Yao JY, Chen JK. TAp63 plays compensatory roles in p53-deficient cancer cells under genotoxic stress. Biochemical and Biophysical Research Communications. 2010; 403: 310–315. https://doi.org/10.1016/j.bbrc.2010.11.025.

[17] Christowitz C, Davis T, Isaacs A, van Niekerk G, Hattingh S, Engelbrecht AM. Mechanisms of doxorubicin-induced drug resistance and drug resistant tumour growth in a murine breast tumour model. BMC Cancer. 2019; 19: 757. https://doi.org/10.1186/s12885-019-5939-z.

[18] Christidi E, Brunham LR. Regulated cell death pathways in doxorubicin-induced cardiotoxicity. Cell Death & Disease. 2021; 12: 339. https://doi.org/10.1038/s41419-021-03614-x.

[19] Linders AN, Dias IB, López Fernández T, Tocchetti CG, Bomer N, Van der Meer P. A review of the pathophysiological mechanisms of doxorubicin-induced cardiotoxicity and aging. Npj Aging. 2024; 10: 9. https://doi.org/10.1038/s41514-024-00135-7.

[20] Hientz K, Mohr A, Bhakta-Guha D, Efferth T. The role of p53 in cancer drug resistance and targeted chemotherapy. Oncotarget. 2017; 8: 8921–8946. https://doi.org/10.18632/oncotarget.13475.

[21] Zhao Y, Gao JL, Ji JW, Gao M, Yin QS, Qiu QL, *et al*. Cytotoxicity enhancement in MDA-MB-231 cells by the combination treatment of tetrahydropalmatine and berberine derived from Corydalis yanhusuo W. T. Wang. Journal of Intercultural Ethnopharmacology. 2014; 3: 68–72. https://doi.org/10.5455/jice.20140123040224.

[22] Luchtel RA, Bhagat T, Pradhan K, Jacobs WR, Jr, Levine M, Verma A, *et al*. High-dose ascorbic acid synergizes with anti-PD1 in a lymphoma mouse model. Proceedings of the National Academy of Sciences of the United States of America. 2020; 117: 1666–1677. https://doi.org/10.1073/pnas.1908158117.

[23] Rueden CT, Schindelin J, Hiner MC, DeZonia BE, Walter AE, Arena ET, *et al*. ImageJ2: ImageJ for the next generation of sci-

entific image data. BMC Bioinformatics. 2017; 18: 529. https://doi.org/10.1186/s12859-017-1934-z.

[24] Osada M, Park HL, Nagakawa Y, Yamashita K, Fomenkov A, Kim MS, *et al*. Differential recognition of response elements determines target gene specificity for p53 and p63. Molecular and Cellular Biology. 2005; 25: 6077–6089. https://doi.org/10.1128/MCB.25.14.6077-6089.2005.

[25] Ciuffoli V, Lena AM, Gambacurta A, Melino G, Candi E. Myoblasts rely on TAp63 to control basal mitochondria respiration. Aging. 2018; 10: 3558–3573. https://doi.org/10.18632/aging.101668.

[26] Komarov PG, Komarova EA, Kondratov RV, Christov-Tselkov K, Coon JS, Chernov MV, *et al*. A chemical inhibitor of p53 that protects mice from the side effects of cancer therapy. Science (New York, N.Y.). 1999; 285: 1733–1737. https://doi.org/10.1126/science.285.5434.1733.

[27] Codelia VA, Cisterna M, Alvarez AR, Moreno RD. p73 participates in male germ cells apoptosis induced by etoposide. Molecular Human Reproduction. 2010; 16: 734–742. https://doi.org/10.1093/molehr/gaq045.

[28] Davidson W, Ren Q, Kari G, Kashi O, Dicker AP, Rodeck U. Inhibition of p73 function by Pifithrin-alpha as revealed by studies in zebrafish embryos. Cell Cycle (Georgetown, Tex.). 2008; 7: 1224–1230. https://doi.org/10.4161/cc.7.9.5786.

[29] Chandrashekar DS, Karthikeyan SK, Korla PK, Patel H, Shovon AR, Athar M, *et al*. UALCAN: An update to the integrated cancer data analysis platform. Neoplasia (New York, N.Y.). 2022; 25: 18–27. https://doi.org/10.1016/j.neo.2022.01.001.

[30] Chen J, Ding ZY, Li S, Liu S, Xiao C, Li Z, *et al*. Targeting transforming growth factor-β signaling for enhanced cancer chemotherapy. Theranostics. 2021; 11: 1345–1363. https://doi.org/10.7150/thno.51383.

[31] Komatsu S, Takenobu H, Ozaki T, Ando K, Koida N, Suenaga Y, *et al*. Plk1 regulates liver tumor cell death by phosphorylation of TAp63. Oncogene. 2009; 28: 3631–3641. https://doi.org/10.1038/onc.2009.216.

[32] Lehmann BD, Bauer JA, Chen X, Sanders ME, Chakravarthy AB, Shyr Y, *et al*. Identification of human triple-negative breast cancer subtypes and preclinical models for selection of targeted therapies. The Journal of Clinical Investigation. 2011; 121: 2750–2767. https://doi.org/10.1172/JCI45014.

[33] Dibra D, Moyer SM, El-Naggar AK, Qi Y, Su X, Lozano G. Triple-negative breast tumors are dependent on mutant p53 for growth and survival. Proceedings of the National Academy of Sciences of the United States of America. 2023; 120: e2308807120. https://doi.org/10.1073/pnas.2308807120.

[34] Cai BH, Chao CF, Lin HC, Huang HY, Kannagi R, Chen JY. A/T gap tolerance in the core sequence and flanking sequence requirements of non-canonical p53 response elements. Journal of Biochemistry. 2016; 159: 563–572. https://doi.org/10.1093/jb/mvw005.

[35] Wang J, Thomas HR, Li Z, Yeo NCF, Scott HE, Dang N, *et al*. Puma, noxa, p53, and p63 differentially mediate stress pathway induced apoptosis. Cell Death & Disease. 2021; 12: 659. https://doi.org/10.1038/s41419-021-03902-6.

[36] Wu KY, Crucho A, Su M, Chen ST, Hung CH, Kou YL, *et al*. Synergistic Anticancer Activity of HSP70 Inhibitor and Doxorubicin in Gain-of-Function Mutated p53 Breast Cancer Cells. Biomedicines. 2025; 13: 1034. https://doi.org/10.3390/biomedicines13051034.

[37] Huang X, Shi D, Zou X, Wu X, Huang S, Kong L, *et al*. BAG2 drives chemoresistance of breast cancer by exacerbating mutant p53 aggregate. Theranostics. 2023; 13: 339–354. https://doi.org/10.7150/thno.78492.

[38] Mariathasan S, Turley SJ, Nickles D, Castiglioni A, Yuen K, Wang Y, *et al*. TGFβ attenuates tumour response to PD-L1 blockade by contributing to exclusion of T cells. Nature. 2018; 554: 544–548. https://doi.org/10.1038/nature25501.

[39] Premkumar K, Shankar BS. TGF-βR inhibitor SB431542 restores immune suppression induced by regulatory B-T cell axis and decreases tumour burden in murine fibrosarcoma. Cancer Immunology, Immunotherapy: CII. 2021; 70: 153–168. https://doi.org/10.1007/s00262-020-02666-w.

[40] Ma XM, Luo YF, Zeng FF, Su C, Liu X, Li XP, *et al*. TGF-β1-Mediated PD-L1 Glycosylation Contributes to Immune Escape *via* c-Jun/STT3A Pathway in Nasopharyngeal Carcinoma. Frontiers in Oncology. 2022; 12: 815437. https://doi.org/10.3389/fonc.2022.815437.

[41] He H, Wang C, Dai Q, Li F, Bergholz J, Li Z, *et al*. p53 and p73 Regulate Apoptosis but Not Cell-Cycle Progression in Mouse Embryonic Stem Cells upon DNA Damage and Differentiation. Stem Cell Reports. 2016; 7: 1087–1098. https://doi.org/10.1016/j.stemcr.2016.10.008.

[42] Mou H, Vinarsky V, Tata PR, Brazauskas K, Choi SH, Crooke AK, *et al*. Dual SMAD Signaling Inhibition Enables Long-Term Expansion of Diverse Epithelial Basal Cells. Cell Stem Cell. 2016; 19: 217–231. https://doi.org/10.1016/j.stem.2016.05.012.

[43] Suzuki D, Pinto F, Senoo M. Inhibition of TGF-β signaling supports high proliferative potential of diverse p63$^+$ mouse epithelial progenitor cells in vitro. Scientific Reports. 2017; 7: 6089. https://doi.org/10.1038/s41598-017-06470-y.